Jpn. J. Appl. Phys. Vol. 35 (1996) pp. 4919–4924
Part 1, No. 9B, September 1996

Time-Dependent Leakage Current Behavior of Integrated $Ba_{0.7}Sr_{0.3}TiO_3$ Thin Film Capacitors during Stressing

Yasuhiro SHIMADA, Atsuo INOUE, Toru NASU, Yoshihisa NAGANO, Akihiro MATSUDA, Koji ARITA, Yasuhiro UEMOTO, Eiji FUJII and Tatsuo OTSUKI

Electronics Research Laboratory, Matsushita Electronics Corporation, Takatsuki, Osaka 569-11, Japan

(Received April 26, 1996; accepted for publication June 28, 1996)

Time-dependent leakage current behavior of integrated $Ba_{0.7}Sr_{0.3}TiO_3$ capacitors accelerated by stresses in excess of operating temperature and voltage was studied. Current-voltage (J-V) studies revealed that the time-dependent leakage current behaviors are different according to the initial conduction process. When the initial leakage current of a fully processed integrated capacitor at high voltages at elevated temperatures is of the Frenkel-Poole emission type, the leakage current increases rapidly with time. The difference in the initial leakage currents is related to the difference in film growth conditions which determine the formation of defects in the films. The time-dependent increase in leakage current is ascribed to a change in the conduction mechanism from the interface-controlled Schottky type to the bulk-related space-charge-limited type due to the accumulation of oxygen vacancies near the cathode as a result of interface barrier lowering and the migration of distributed oxygen vacancies across the film.

KEYWORDS: ferroelectric, integrated ferroelectrics, ferroelectric memory, leakage current, conduction mechanism

1. Introduction

Because of the extensive evolution in integration technology of high-dielectric-constant ferroelectric materials such as $Ba_{1-x}Sr_xTiO_3$ (BST), $Pb_xZr_{1-x}TiO_3$ (PZT), and $SrBi_2Ta_2O_9$ (SBT),[1] integration of ferroelectric capacitors has been regarded as the most advanced technology to minimize and simplify the device structure of dynamic random access memories (DRAMs) beyond gigabit scales, as well as to realize nonvolatile ferroelectric memories.[2,3] For practical memory applications of these materials, their electrical properties must be properly understood and kept stable for a period of operating time comparable with the minimum life of peripheral incorporated silicon devices. Among several factors associated with capacitor reliability, degradation of the insulation resistivity is the most crucial issue because it causes a change in stored charge in memory capacitors for a certain period of the refreshing cycle due to an increase in leakage current during long-term memory operation. Therefore the minimization of the variation in leakage current is a fundamental issue for memory applications of these ferroelectric materials.

The gradual increase in leakage current associated with a degradation of the insulation resistivity is commonly observed when temperature and dc voltage stresses are applied to ferroelectric capacitors for a certain period of time.[4] Even under less excessive temperature and voltage stresses close to normal device operating conditions, much below the critical onset of instant breakdown, a slight increase in leakage current is still observed. Under excessive temperature and voltage stresses close to the occurrence of instant dielectric breakdown, an anomalous increase in leakage current followed by eventual breakdown is observed. A quantitative model based on defect chemistry for the degradation in multilayer ceramic capacitors has been proposed.[5] Similar phenomena have been observed in $BaTiO_3$, BST, and PZT during the latter part of the life terminated by the eventual breakdown.[6–10]

In this work, time-dependent leakage current behavior of integrated BST capacitors is studied. The sample capacitors were separated into two types according to different film preparation process routes. The temperature dependence of current-voltage (J-V) characteristics of each type of capacitors is studied to reveal the predominant conduction mechanism under a given stress. The influence of the initial predominant conduction mechanism on the change in the J-V characteristics during stressing is studied. A possible scenario which describes the change in the conduction mechanism during stressing is discussed.

2. Experimental

In the present experiments, $Ba_{0.7}Sr_{0.3}TiO_3$ films were prepared by metal-organic decomposition (MOD) using a homogeneous solution containing a stoichiometrically correct 6 wt% BST precursor. The MOD solution was spin-coated to form BST films on 300-nm-thick Pt-deposited silicon wafers in which digital/analog filtering ICs are fabricated.[11,12] The BST films were then annealed at a high temperature in atmospheric oxygen either with a rapid temperature ramp rate for sample A or with a slow temperature ramp rate for sample B. The total thickness of the BST films was about 185 nm for both types of capacitors after annealing. After the high temperature annealing, Pt electrodes of 150 nm were deposited on the crystallized BST to form a metal-ferroelectric-metal structure and a number of photomasked capacitors with the size of $200 \times 200\,\mu m^2$ were patterned in a plasma etcher. Subsequently, the capacitors were covered with interlayer silicon dioxide films formed by chemical vapor deposition and the interlayer films were etched in a plasma to form contact openings to interconnect between the capacitors and underlaying peripheral transistor circuits. After the metallization with sputtered aluminum, interconnect patterns were formed by wet chemical processing. After postmetallization annealing in forming gas, SiN films were deposited for passivation and then bonding pad openings were formed by dry etching. Since the leakage current of ferroelectric capacitors without proper barriers is very sensitive to moisture,[8] the SiN passivation is inevitable to ensure the reliability of all measurements in this experiment.

The *J-V* curves of the fully processed capacitors were measured on a hot stage with a HP4145B semiconductor parameter analyzer at different temperatures in the range of 300–423 K. Time-dependent leakage current behavior at elevated temperatures and high voltages was monitored with the same instruments. Long-term electrical degradation for up to 1500 h was evaluated by the leakage current measured at 3 V at room temperature before and after the integrated capacitors were subjected to high-temperature and high-voltage stresses.

3. Results

3.1 *Initial J-V characteristics*

After the completion of integration processing, *J-V* measurements were made on type A and type B capacitors before stressing. Since the film growth process influences the microstructure of the grain size, grain boundaries, defect distribution, and interface states, the nature of bulk-controlled conduction in the capacitors may change depending on the film growth conditions.

First we studied the electrode interface-controlled current. Figure 1 shows the *J-V* curves for a temperature range of 300–423 K of type A and type B capacitors after the completion of the integration process. The linear behavior of the curves at high voltages indicates the Schottky current and the slope yields the dynamic dielectric constant of the ferroelectric.[13] Since both types of capacitors show the same behavior at high voltages, we can assume that the interface barrier height and the dielectric constant of type A capacitors are identical with those of type B capacitors.

Secondly, we studied the bulk-controlled conduction

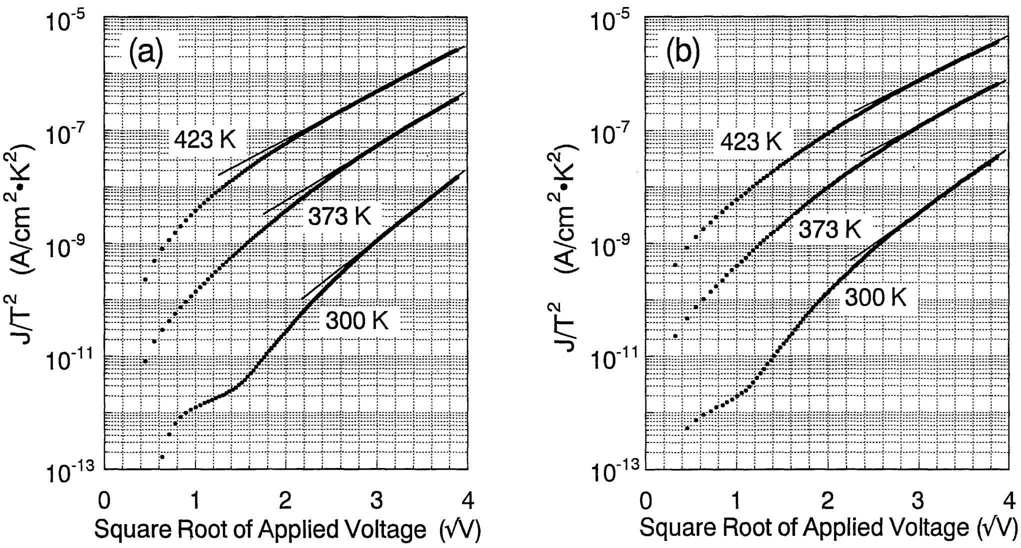

Fig. 1. Initial *J-V* curves on a log *J* vs $\sqrt{V}$ plot measured at 300, 373, and 423 K before stressing of (a) a type A capacitor annealed with a rapid ramp rate and of (b) a type B capacitor annealed with a slow ramp rate.

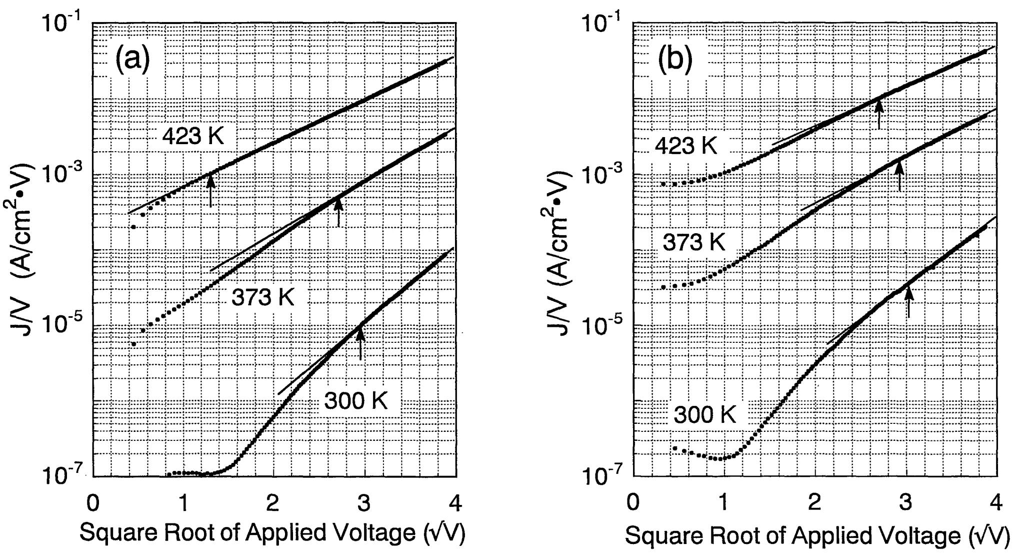

Fig. 2. Initial *J-V* curves on a log J/V vs $\sqrt{V}$ plot measured at 300, 373, and 423 K before stressing of (a) a type A capacitor annealed with a rapid ramp rate and of (b) a type B capacitor annealed with a slow ramp rate. The onset voltage of the linear behavior is indicated by arrows on each curve.

in BST films. In the presence of a large amount of defects in ferroelectric films, the leakage current at high temperatures at high voltages is frequently referred to as the Frenkel-Poole (F-P) conduction. Figure 2 shows $\log J/V$ vs $\sqrt{V}$ curves to reveal the J-V behavior subject to the F-P conduction. Arrows in Fig. 2 indicate the points of approximate onset of the linear behavior on each curve. Unlike the curves in Fig. 2(b) for a type B capacitor, the curves in Fig. 2(a) for a type A capacitor show that the onset voltage of linear behavior is lowered as the temperature is elevated. When the temperature is 423 K, for instance, the approximate onset voltage for the type A capacitor is 1.7 V while that for the type B capacitor is 7.0 V. At high temperatures, therefore, the leakage current of type A capacitors appears to be more strongly governed by the F-P mechanism even at low voltages than in type B capacitors. Since the F-P emission is due to field-enhanced thermal excitation of trapped carriers, we assume that type A capacitors are richer in Frenkel-type defects, both oxygen vacancies, metal vacancies, and interstitial metals, than type B capacitors.

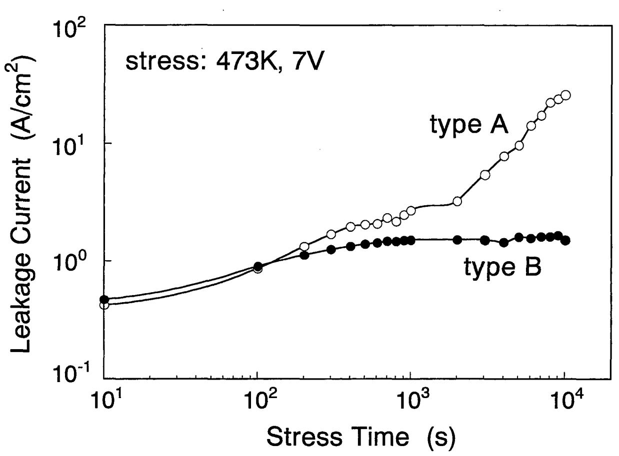

Fig. 3. Time-dependent leakage current behavior of integrated BST capacitors during stressing at 7 V and 473 K. The upper curve is for a type A capacitor and the lower curve is for a type B capacitor.

3.2 *Time-dependent leakage current behavior during stressing*

Figure 3 shows time-dependent leakage current behaviors during stressing with 7 V at 473 K for 10^4 s. At the beginning of stressing, both types of capacitors exhibited the same leakage current level. For the next hundred seconds, the leakage currents show transient increases without any transient decrease due to electrical charge hopping or dielectric polarization as seen in PZT[4,7] and BST,[14] or due to charge absorption relaxation at distributed grain boundaries in $SrTiO_3$ and $BaTiO_3$,[15] because the applied voltage, corresponding to a field of about 380 kV/cm, is much higher than the ohmic voltage region below 50 kV/cm.[4,16] After the transient regime the type A capacitor shows a further gradual increase in leakage current with time, whereas the type B capacitor exhibits a stable leakage current after a stress time of 10^3 s. These time-dependent studies indicate that the leakage current under an excessive stress show different behaviors depending on the BST film growth conditions, even if the initial leakage currents are in the same level.

3.3 *J-V characteristics before and after stressing*

After being subjected to the high-temperature high-voltage stress for 10^4 s, J-V characteristics of both types of capacitors were again measured at room temperature, as shown in Fig. 4. The leakage current of the type A capacitor increased by 4 orders of magnitude from the original level, whereas that of the type B capacitor increased by 2 orders of magnitude. When we assume the leakage current to be limited only by interface thermionic emission at the cathode, the leakage current at a given temperature is determined by the interface barrier height and the dielectric constant of the ferroelectric. Despite the increase in leakage current after stressing for both types of capacitors, the slopes at high voltages in terms of the dielectric constant are nearly identical to their

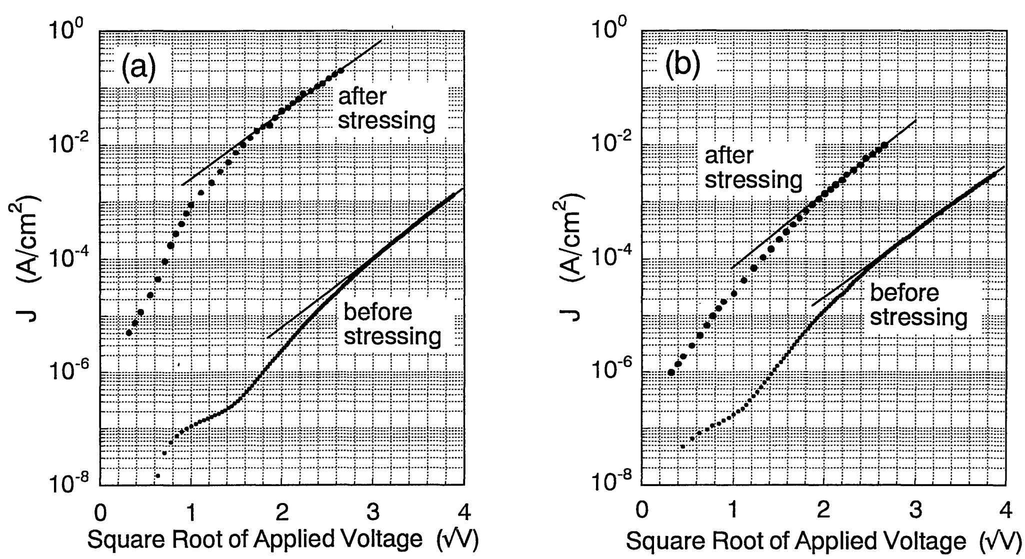

Fig. 4. J-V curves on a $\log J/V$ vs $\sqrt{V}$ plot of (a) a type A capacitor after stressing is larger than that of (b) a type B capacitor measured at room temperature before and after stressing at 7 V and 473 K for 10^4 s.

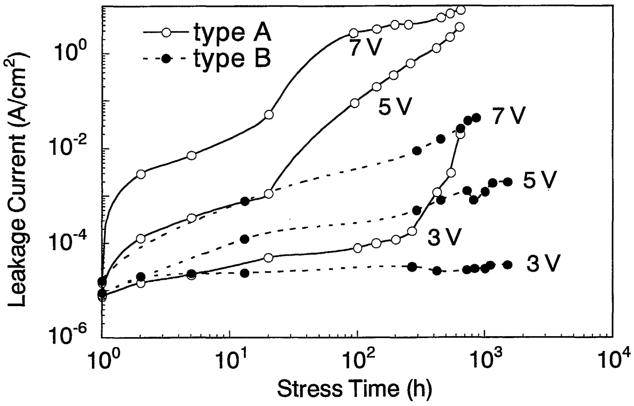

Fig. 5. Variations in leakage current with stress time. The samples were subjected to stresses of positive applied voltages of 3, 5, and 7 V at 423 K for up to 1500 h. The leakage currents were measured at 3 V at room temperature.

original values. This result implies the lowering of the interface barrier height due to the stress. Based on the Schottky model, the lowering of the barrier height due to the stress is then calculated to be approximately 0.2 eV for the increase in leakage current of the type A capacitor and 0.1 eV for that of the type B capacitor.

3.4 *Voltage dependence of long-term behavior*

Long-term electrical degradation of the integrated capacitors was evaluated from the variation in leakage current at room temperature at 3 V after being subjected to a temperature of 423 K at different bias voltages. The stress voltage was chosen to be 3, 5, and 7 V to simulate the possible operating voltage range for standard-use conditions. The leakage currents were measured at proper intervals during stressing for up to 1500 h. As shown in Fig. 5, the variation in leakage current has a strong dependence on the applied voltage for both types of capacitors. For an applied voltage of 3 V, the leakage current in a type B capacitor is very stable for up to 1500 h, whereas in a type A capacitor an anomalous increase in leakage current appears after 100 h. The stress voltage in this region is much lower than the onset of the F-P behavior in type B capacitors, while it overlaps with the onset of the F-P behavior in type A capacitors as seen in Fig. 1. When the stress voltage is increased to 5 or 7 V, which is higher than the onset voltages of F-P emission in both types of capacitors, the leakage currents in type A capacitors increase faster than those in type B capacitors. Since the initial presence of the F-P conduction is inevitable for the time-dependent increase in leakage current, it is concluded that the F-P mechanism is associated with a time-dependent change in the nature of the conduction process.

4. Discussion

Since the F-P conduction is responsible for the time-dependent increase in leakage current, and the most likely traps for this mechanism are oxygen vacancies, we here postulate that the time-dependent change in leakage current is associated with the presence of oxygen vacancies.[4,5] Many groups to date have pointed out the importance of the role of oxygen vacancies in the time evolution of the bulk-related leakage current of ferroelectric capacitors, i.e., a field-driven redistribution of oxygen vacancies in the films would result in the formation of a forward-biased *p*-*n* junction.[6,10,17] However, their arguments are limited in the change of the leakage current in the bulk. When the leakage current under consideration is originally predominated by the interface-controlled Schottky emission, we must take into account the change in leakage current at the interface as well as in the bulk.

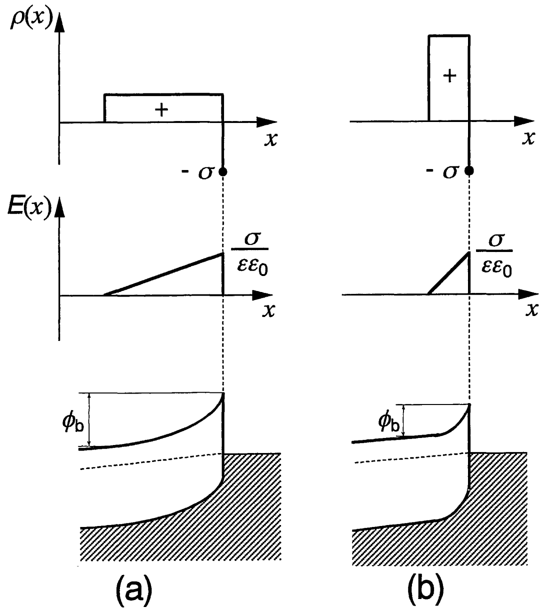

Fig. 6. Comparison of the charge distribution ρ, electric field E, and energy band variation as a function of the direction x near the cathode of a BST capacitor (a) before and (b) after stressing.

When we denote the interface-controlled leakage current by J_i and the bulk-controlled current by J_b, we have $J_i = J_b$ in the steady state. Current continuity at the interface in the steady state requires that charge accumulation takes place at the surface inside the metallic cathode if nonequilibrium current discontinuity exists across the interface, which means that the electric field distribution is adjusted until current continuity is established. Current continuity then leads to $\varepsilon\varepsilon_0 E = \sigma$, where E is the electric field at the surface inside the ferroelectric, σ is the charge accumulation at the surface inside the metallic cathode per unit area, ε_0 is the dielectric constant of vacuum, and ε is the dielectric constant of ferroelectric. To compensate the accumulated charge σ, oxygen vacancies distributed near the interface are positively ionized. As a result, a built-in potential ϕ_b is formed at the interface so as to control the current J_i.

In our BST capacitors, the concentration of oxygen vacancies in type A capacitors is estimated to be greater than that in type B capacitors because of the difference in the onset of linear behaviors in Fig. 2 and in the voltage dependence of the long-term leakage current behaviors in Fig. 5. When the temperature is elevated, oxygen vacancies initially distributed across the film are thermally activated and begin to migrate toward the cathode under high fields. Finally, the oxygen vacancies accumulate

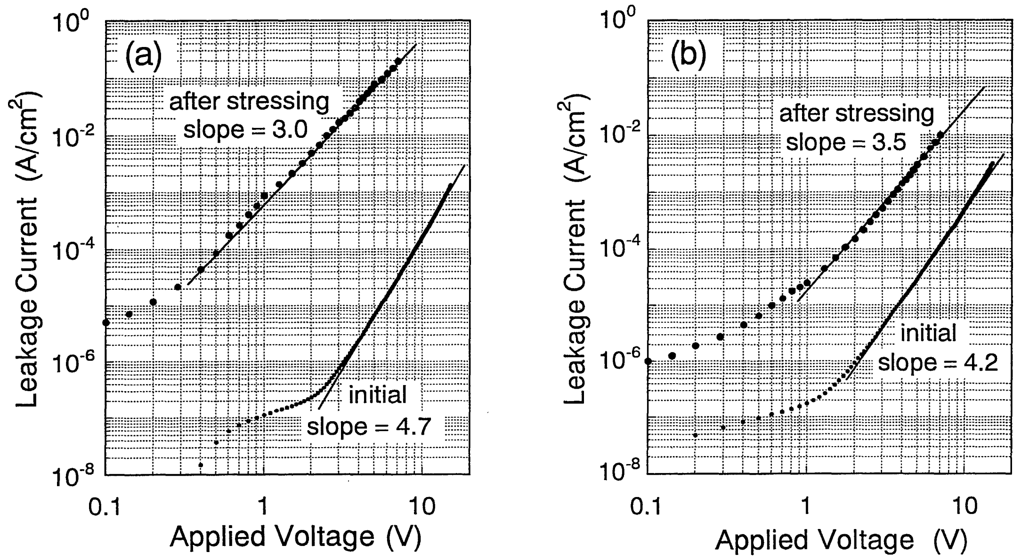

Fig. 7. Curves on a log J- log V plot for (a) a type A capacitor and (b) a type B capacitor measured at room temperature before and after stressing at 7 V and 473 K for 10^4 s.

near the cathode. Since the interface barrier originates from the built-in potential primarily formed between accumulated charge at the interface and ionized oxygen vacancies in the depleted region near the interface, the barrier height is lowered as the depletion region is reduced due to accumulation of oxygen vacancies at the cathode, as illustrated in Fig. 6. Therefore, the increase in leakage current in the presence of excessive stress is more likely to occur in type A capacitors than in type B capacitors.

As a result of the barrier lowering at the cathode, the bulk-controlled conduction appears to be predominant. If we assume a complete diffusion of oxygen vacancies across the film, the leakage current behavior should be similar to the space-charge-limited current process with the trap-free square law.[18] From the experimental result for a stress of 7 V and 423 K applied for 10^4 s, both types of capacitors exhibited a decrease in the slope of the linear behavior toward a slope of 2 on log J vs log V plots in Fig. 7. This result supports that the contribution of the space-charge-limited current with the trap-free square law becomes predominant during stressing. Therefore we conclude that the increase in leakage current of our integrated BST capacitors is caused by a change in the conduction process from the interface-controlled Schottky type to the bulk-related space-charge-limited type due to the redistribution of oxygen vacancies across the film during stressing.

5. Conclusions

We have shown the J-V characteristics of integrated BST capacitors and their time-dependent behavior under excessive temperature and voltage stresses for up to 1500 h. The J-V behaviors indicated a strong dependence on the film growth conditions. After excessive stressing, J-V curves indicated the lowering of barrier height and an asymptotic fit to the space-charge-limited process. From the difference in the onset of the Frenkel-Poole behavior between two types of capacitors with different film growth processes, the presence of oxygen vacancies was concluded to be responsible for the change in leakage current with time. The increase in leakage current is thus caused by the lowering of interface barrier height as a result of the accumulation of oxygen vacancies at the cathode, and the space-charge-limited current becomes predominant due to the migration of oxygen vacancies across the film.

Acknowledgements

The authors thank all their colleagues whose support encouraged this work. The authors also thank Professor C. A. Paz de Araujo of the University of Colorado at Colorado Springs for his valuable advice, and the staff of Symetrix Corporation for their continuous support.

1) Y. Shimada, Y. Nagano, E. Fujii, M. Azuma, Y. Uemoto, T. Sumi, Y. Judai, S. Hayashi, N. Moriwaki, J. Nakane, T. Otsuki, C. A. Paz de Araujo and L. D. McMillan: Integr. Ferroelectr. **11** (1995) 229.
2) C. A. Araujo, L. D. McMillan, B. M. Melnick, J. D. Cuchiaro and J. F. Scott: Ferroelectrics **104** (1990) 241.
3) R. Moazzami, C. Hu and W. H. Shepherd: IEEE Electron Device Lett. **11** (1990) 454.
4) H. Hu and S. B. Krupanidhi: J. Mater. Res. **9** (1994) 1484.
5) R. Waser: J. Am. Ceram. Soc. **73** (1990) 1654.
6) S. B. Desu and I. K. Yoo: J. Electrochem. Soc. **140** (1993) L133.
7) X. Chen, A. I. Kingon, L. Mantese, O. Auciello and K. Y. Hsieh: Integr. Ferroelectr. **3** (1993) 355.
8) X. Chen, A. I. Kingon, H. N. Al-Shareef, K. R. Bellur, K. Gifford and O. Auciello: Intergr. Ferroelectr. **7** (1995) 291.
9) K. Numata, Y. Fukuda, K. Aoki and A. Nishimura: Jpn. J. Appl. Phys. **34** (1995) 5245.
10) D. J. Wouters, G. Willems, G. Groeseneken, H. E. Meas and K. Brooks: Integr. Ferroelectr. **7** (1995) 173.
11) K. Arita, E. Fujii, Y. Shimada, Y. Uemoto, M. Azuma, S. Hayashi, T. Nasu, A. Inoue, A. Matsuda, Y. Nagano, S. Katsu, T. Otsuki, G. Kano, L. D. McMillan and C. A. Paz de Araujo: IEICE Trans. Electron. **E77-C** (1994) 392.
12) K. Arita, E. Fujii, Y. Shimada, Y. Uemoto, T. Nasu, A. Inoue, A. Matsuda, T. Otsuki and N. Suzuoka: Jpn. J. Appl. Phys.

33 (1994) 5397.
13) Y. Shimada, A. Inoue, T. Nasu, K. Arita, Y. Nagano, A. Matsuda, Y. Uemoto, E. Fujii, M. Azuma, Y. Oishi, S. Hayashi and T. Otsuki: Jpn. J. Appl. Phys. **35** (1996) 140.
14) W. Y. Hsu, J. D. Luttmer, R. Tsu, S. Summerfelt, M. Bedekar, T. Tokumo and J. Nulman: Appl. Phys. Lett. **66** (1995) 2975.
15) R. Waser and M. Klee: Proc. 3rd Int. Symp. Integr. Ferroelectr., Colorado Springs, 1991, p. 288.
16) G. M. Rao and S. B. Krupanidhi: J. Appl. Phys. **75** (1994) 2604.
17) T. Baiatu, R. Waser and K.-H. Härdtl: J. Am. Ceram. Soc. **73** (1990) 1654.
18) M. A. Lampert and P. Mark: *Current Injection in Solids* (Academic Press, New York, 1970).